ARTICLE Libri Oncol., Vol. 36 (2008), No 1-3, 1 – 10

GENITOURINARY CANCER: THE POTENTIAL ROLE OF IMAGING

TVRTKO HUDOLIN[1] and HEDVIG HRICAK[2]

[1]Departments of Radiology and Urology, Memorial Sloan-Kettering Cancer Center, New York, NY, USA
[2]Department of ‡Urology, KBC Zagreb, Zagreb, Croatia

Summary

Imaging is an essential part of the management of patients with genitourinary cancers. Imaging is necessary for diagnosis, treatment selection and planning, applying minimally invasive image-guided techniques, assessment of response to treatment, and post-treatment follow-up. With advances in technology, imaging now comprises far more than descriptive anatomy. In the next decade anatomic, functional and molecular imaging information will increasingly be combined to achieve more accurate disease characterization and better patient care. In this review we present standard as well as some new imaging methods used in patients with kidney and prostate cancer.

KEYWORDS: *imaging, prostate cancer, kidney cancer, computed tomography, magnetic resonance imaging, ultrasonography, scintigraphy*

GENITOURINARNI KARCINOMI: POTENCIJALNA ULOGA OSLIKAVANJA

Sažetak

Oslikavanje je sastavni dio liječenja bolesnika s genitourinarnim karcinomima. Oslikavanje je nužno za dijagnozu bolesti, izbor i planiranje terapije, te vođenje minimalno invazivnih tehnika liječenja, procjenu odgovora na terapiju, te praćenje bolesnika nakon liječenja. S napretkom tehnologije oslikavanje je danas puno više od deskriptivne anatomije. U sljedećoj dekadi kombinirat će se informacije anatomskog, funkcionalnog i molekularnog oslikavanja s ciljem postizanja što bolje karakterizacije bolesti, a samim time i boljeg liječenja bolesnika. U ovom članku prikazat ćemo standardne i neke nove metode oslikavanja koje se primjenjuju kod bolesnika s karcinomom bubrega i karcinomom prostate.

KLJUČNE RIJEČI: *oslikavanje, karcinom prostate, karcinom bubrega, kompjutorizirana tomografija, nuklearna magnetna rezonancija, ultrazvuk, scintigrafija*

IMAGING OF KIDNEY CANCERS

Kidney cancers represent 2-3% of all cancer cases. The disease is nearly twice as common in men as in women and occurs most frequently in individuals between 60 and 70 years of age (1). The etiology of the disease is not clear, and although studies have identified a number of factors that may be related to kidney cancer, cigarette smoking is the only established risk factor (2). Since the introduction of ultrasonography and computerized tomography (CT), the rate of detection of kidney tumors has increased substantially. The percentage of kidney cancers diagnosed incidentally has increased from 17% three decades ago to 58% in recent years (3).

In some patients, the tumors detected are malignant and demand surgical treatment. However, in other patients with benign tumors, surgery may represent over-treatment. Furthermore, malignant renal tumors with different histological subtypes have different prognoses. The most common renal

cell carcinoma (RCC) subtypes are clear cell (accounting for approximately 60%), papillary (accounting for 7-14%), chromophobe (accounting for 6-11%), oncocytoma (accounting for 7-10%) and collecting duct and medullary (accounting for <1%) (4). The most aggressive tumors are collecting duct (Bellini duct) and medullary carcinoma, followed by the clear-cell type. Papillary and chromophobe cell types have favorable prognoses compared with the clear-cell type and oncocytoma is considered to be a benign neoplasm (4, 5).

The main role of imaging in patients with kidney cancer is to define the location and extent of the kidney mass. Although imaging modalities can differentiate solid from cystic masses, it is much more challenging to predict the nature of solid renal tumors. Although studies have suggested that certain imaging features may be associated with specific renal cortical tumor subtypes, there are no well-established imaging criteria for differentiating between these subtypes.

Figure 1. Patient with a renal mass that proved to be clear cell carcinoma at surgery. Color Doppler US image shows marked intratumoral vascularity, indicating the solid nature of the tumor.

Ultrasonography

Ultrasound is often a first-line approach for differentiating between solid and cystic kidney lesions (Figure 1). If a solid lesion is found on ultrasound, CT should be used for local staging and to search for metastatic disease. If a cystic lesion is not simple (avascular and completely anechoic, with a thin, imperceptible wall, posterior enhancement, and a round or oval shape) further evaluation with CT and/or magnetic resonance imaging (MRI) is recommended (6). Although ultrasound is insufficient for differentiating the histological subtype of the tumor, a recent study showed that vascular flow detected by color Doppler ultrasonography was strongly associated with conventional clear cell histology (Figure 1, 2) (7). Compared to unenhanced color Doppler imaging, ultrasound with microbubble-based contrast agents that enhance blood vessels enables better discrimination between benign and malignant small renal masses (8).

CT

For differentiating between solid renal tumors types, the most consistent and useful imaging characteristic is probably the degree of enhancement. Clear cell RCCs have complex findings on CT, often demonstrating a mixed enhancement pattern of both hypervascular soft-tissue components and low-attenuation areas that repre-

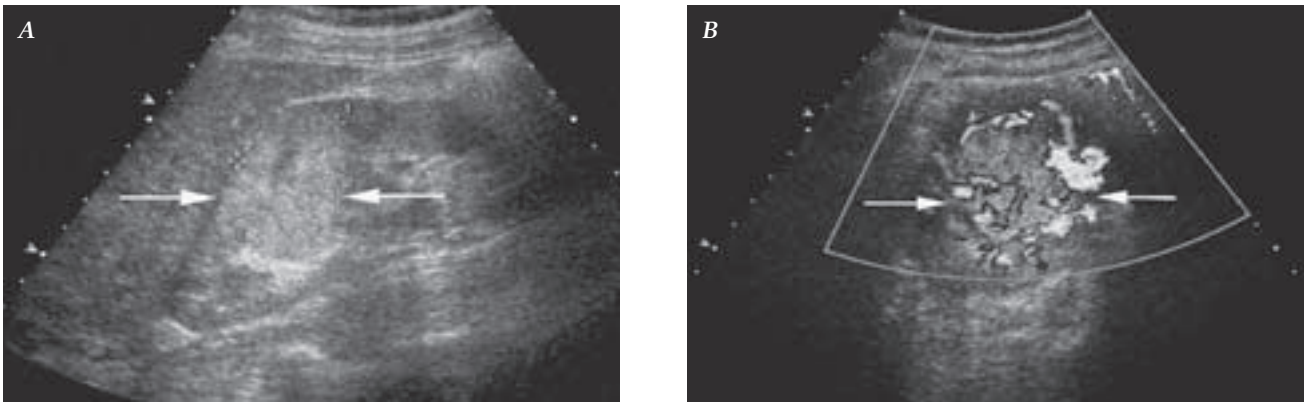

Figure 2. A patient with renal cell carcinoma of the clear cell type. (A): Grayscale ultrasound image shows a homogeneous solid lesion (arrows). (B): Color Doppler ultrasound image shows marked tumor vascularity (arrows).

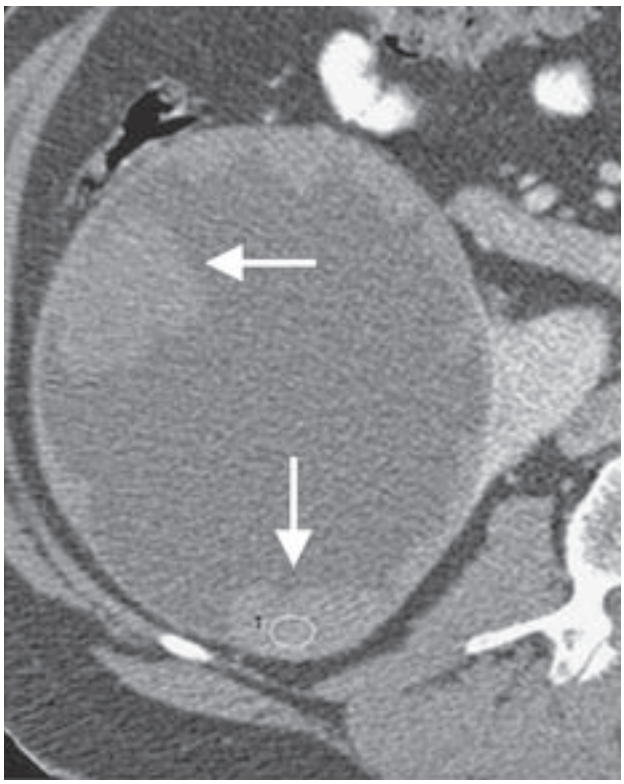

Figure 3. A patient with a palpable right renal mass that proved to be papillary renal cell carcinoma. Contrast-enhanced CT demonstrates a large cystic lesion with enhancing solid vegetations (arrows). Image reprinted from: Zhang J, Lefkowitz RA, Bach A. Imaging of kidney cancer. Radiol Clin North Am 2007;45(1): 119-47.

sent necrotic or cystic changes (9). Some CT findings that are found in clear cell carcinoma can also be seen in oncocytoma (10). The papillary renal cell carcinomas are typically less vascular, and most commonly show either homogeneous or peripheral enhancement (Figure 3) (11). Chromophobe renal cell carcinomas are more variable in their degrees and patterns of enhancement (9).

The accuracy of CT in defining the extent of tumor preoperatively (i.e., in staging) has been reported to be as high as 90%, making it the imaging modality of choice for most patients (12). CT has some limitations, mainly in the evaluation of lymph node involvement, which is assessed based on lymph node size. The enlargement of lymph nodes to a diameter greater than 2 cm is almost always a sign of metastasis, but lymph nodes between 1 and 2 cm in diameter may also be caused by reactive hyperplasia (13). Multislice CT, with its excellent temporal resolution, has been found to be useful for detecting the presence and extent of inferior vena cava invasion (14).

MRI

MRI has a few advantages in the imaging of kidney cancers compared to CT and is, therefore, the method of choice in selected patients. The accuracy of detection and differentiation of cystic and solid renal lesions on MRI is comparable and at times superior to that on CT (15). MRI can also be used in patients with renal failure or reduced nephrons, or in patients who are allergic to iodine-based contrast agents used with CT. Because of its superior soft tissue contrast, MRI is also reliable for evaluating small renal masses (16).

On T1-weighted images solid renal tumors are typically isointense or slightly hypointense. Rarely, if they contain a lipid component or hemorrhage, they may demonstrate hyperintensity (17, 18). Renal cortical tumors tend to be mildly hyperintense on T2-weighted images and show variable enhancement on dynamic contrast-enhanced images (17, 19). A recent study showed that clear cell carcinomas are hyperintense and heterogenous on T2-weighted images and that on dynamic contrast-enhanced images, papillary cell carcinomas demonstrate less and delayed enhancement compared with the clear cell type (20).

In some cases MRI allows a more detailed assessment of cystic masses than is possible with CT and may show additional septa, thickening of the wall and/or septa, or enhancement - findings that may affect patient management (21).

Nuclear Scintigraphy

Positron emission tomography (PET) is advancing the imaging of many primary and metastatic cancers. Most malignant tumors demonstrate enhanced glucose uptake, which makes them suitable for PET imaging using the glucose analog fluorodeoxyglucose (^{18}F-FDG). However, the use of ^{18}F-FDG PET in the imaging of urological tumors is hampered by the urinary excretion of the tracer and, in some urological cancers, variable uptake of the tracer. Thus, although ^{18}F-FDG PET has a limited role in the initial diagnosis of renal tumors, it can be useful for the detection of local recurrence and distant metastases (e.g., visceral, lymph node and bony metastases) (22).

^{18}F-Fluoromisonidazole (^{18}F-FMISO) is a hypoxia marker and 3′-Deoxy-3′-18F-fluorothymidine (^{18}F-FLT) is a marker of cellular proliferation. Studies have shown that uptake of both of these tracers is higher in tumors than in normal tissue, but more data are needed to validate the roles of these tracers in the imaging of kidney cancer. A recent study found that radiolabeled G250, a monoclonal antibody to carbonic anhydrase IX antigen, targeted clear cell carcinoma with high sensitivity and specificity (23). Further studies are needed to verify these new and exciting results.

Conclusion

CT is generally the imaging modality of choice for the evaluation of renal tumors, while ultrasound and MRI function as valuable problem-solving tools. The role of PET in the imaging of kidney cancer is expected to increase as new tracers are developed and validated.

IMAGING OF PROSTATE CANCER

Prostate cancer is the most commonly diagnosed cancer and the second leading cause of cancer death among men in industrialized countries. The incidence of prostate cancer increases with advancing age, reaching approximately 60% in 60-year-old men (24).The biological behavior of prostate cancer varies widely. In many patients the disease is indolent, while in many others it poses a substantial threat to health and life. A wide array of treatment options is available, and determining which treatment is best for an individual patient is not easy. Accurate characterization of the cancer is essential for appropriate treatment selection. The major objective of prostate cancer imaging is to supplement clinical and pathological data (e.g., the clinical or pathological stage, the Gleason score and the serum PSA level) (25,26) to achieve more precise disease characterization before and after treatment. In addition, with advances in technology, imaging is becoming a tool for guiding local therapies such as radiofrequency ablation, cryotherapy and high-intensity focused ultrasound (27).

Transrectal Ultrasound and CT

Transrectal ultrasound alone has limited utility for identifying prostate cancer, and therefore it has been used mainly to guide needle biopsy and brachytherapy seed implant (28). Real-time contrast-enhanced color Doppler ultrasound for visualization of focal lesions (Figure 4) and elastography for the assessment of tissue elasticity are new techniques which may improve prostate cancer detection, grading and staging (29-31). However, further clinical trials are needed to determine the promise of these new ultrasound techniques. CT has relatively poor soft-tissue resolution in the pelvis and therefore is not a modality of choice for primary prostate cancer. It is recommended that CT should be used only in patients with PSA >20 ng/mL, Gleason sum >7 and/or clinical stage T3 or higher (32). CT can be useful as a baseline examination in high-risk patients with clinically apparent, grossly advanced local disease (gross extracapsular disease, gross seminal vesicle invasion, or invasion of surrounding structure including bladder, rectum, levator ani muscles, or pelvic floor (33). For diagnosis of bone metastases CT is inferior to MRI and bone scans (34).

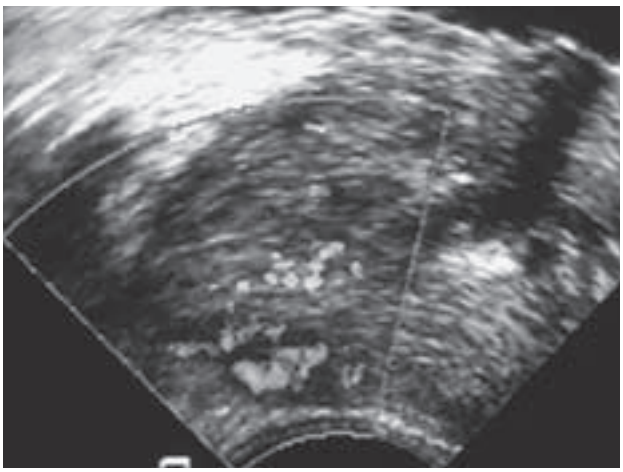

Figure 4. Color Doppler transrectal ultrasound image in a patient with prostate cancer demonstrates a hypoechoic lesion in the right peripheral zone of the prostate, with marked vascularity.

MRI

Due to its superb soft-tissue resolution, MRI can show the zonal anatomy of the prostate as well as the broader pelvic anatomy in detail. It is therefore the modality of choice for the detection and staging of local prostate cancer (Figure 5). MRI can be used to detect extracapsular extension (Figure 6), seminal vesicle invasion, and adjacent organ invasion. Many technological advances have

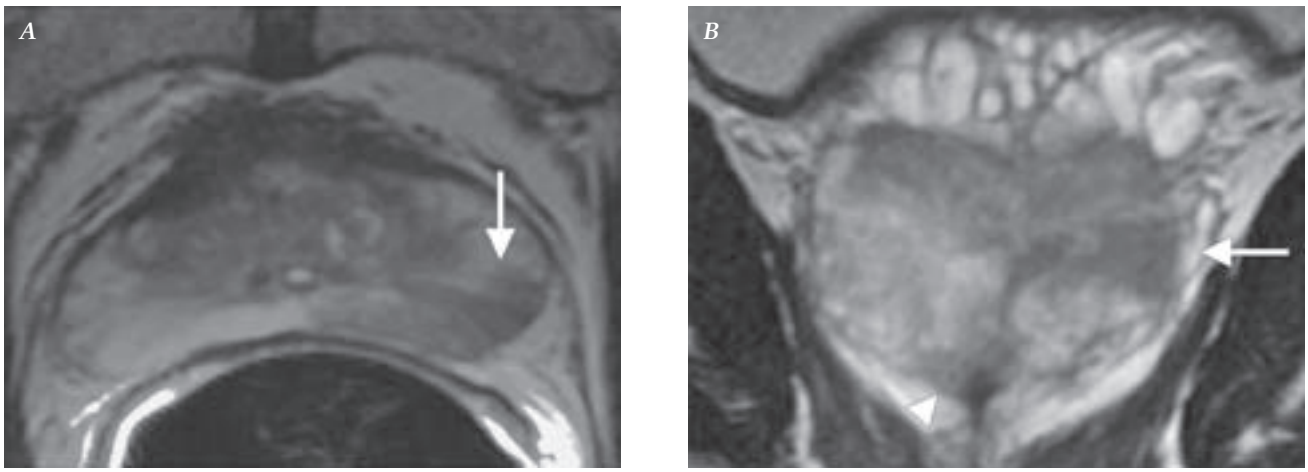

Figure 5. Clinical T1c non-palpable lesion. Endorectal MR images from a patient with non-palpable, clinical stage T1c prostate cancer. Axial (A) and coronal (B) images show a large lesion in the left peripheral zone (arrows); coronal image (B) also shows a second lesion (arrowhead) in the right apex.

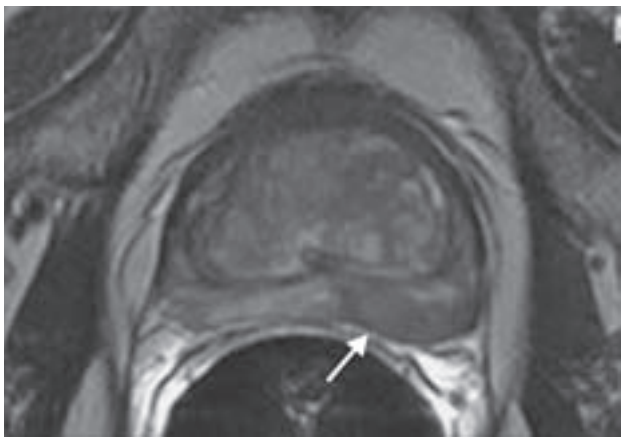

Figure 6. Axial endorectal MR image in a patient with prostate cancer shows a large lesion in the left peripheral zone (arrow) with asymmetry of the neurovascular bundles that is suggestive of early extracapsular extension.

been developed recently in the field of MRI, such as MR spectroscopic imaging (MRSI), dynamic contrast-enhanced MRI (DCE-MRI) and diffusion-weighted imaging (DWI). These new techniques enable anatomic and functional evaluation of the prostate and prostate cancer. Each technique has advantages and disadvantages. In the future, optimal use of MRI will most likely involve the combination of all or some of the various techniques.

Conventional MRI of the prostate typically includes axial T1-weighted imaging of the pelvis for evaluation of pelvic adenopathy, osseous lesions and post-biopsy artifacts in the prostate, as well as small-field, thin-section, high-resolution T2-weighted imaging of the prostate in three orthogonal planes for the detection and localization of prostate tumors. Prostate cancer typically manifests as focal decreased signal on T2-weighted imaging (Figure 5-6), but these changes are not specific for prostate cancer and may also be caused by certain benign conditions, such as prostatitis, or by post-biopsy changes. Nonetheless, conventional MRI has been shown to contribute significant incremental value to both digital rectal examination and transrectal ultrasound-guided biopsy in cancer detection and localization in the prostate (35). In addition, conventional MRI is capable of demonstrating local prostate recurrence after surgery (Figure 7) (36).

MRSI is an established advanced imaging technique for metabolic evaluation of the prostate gland. The addition of MRSI to conventional MRI can significantly improve the accuracy of prostate cancer localization and decrease interobserver variability (37,38). This technique displays concentrations of metabolites in prostatic tissue. The normal prostate contains high levels of citrate and low levels of choline. When cancer is present the citrate level is diminished due to increased energy consumption, and the choline level is elevated owing to a high phospholipid cell membrane turnover in the proliferating malignant tissue. In addition, the level of polyamines, another secretory product of the prostate, decreases in the presence of prostate cancer. In practice, an increased (choline+polyamin es+creatine) to citrate ratio is used to distinguish

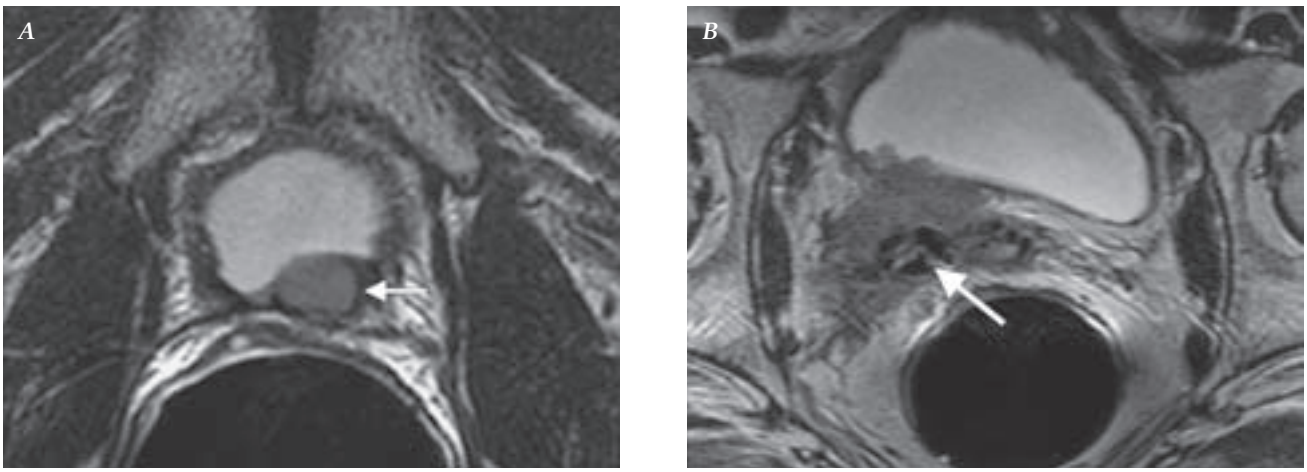

Figure 7. Endorectal MR images from two patients with prostate cancer recurrence after surgery. (A): Axial image shows a small lesion (arrow) at the bladder base. (B): Axial image shows a large tumor recurrence around three surgical clips (arrow).

prostate cancer from healthy tissue on MRSI (39). (Previously, the polyamine peak could not be resolved, and so the [choline+creatine]/citrate ratio was used.) MRSI may provide an indication of tumor aggressiveness, as one study showed that the (choline + creatine)/citrate ratio tended to increase with increasing Gleason scores (40).

DWI is an MRI technique that measures the Brownian motion of water molecules in biologic tissues. Mean apparent diffusion coefficient values for prostate cancer are lower than those for benign prostate tissue, although they overlap substantially (41,42). The combination of T2-weighted imaging and DWI has been found to perform better than T2-weighted imaging alone in the detection of significant prostate cancer (i.e., cancer with a Gleason score of at least 6 and a diameter > 4 mm) within the peripheral zone (43). In addition, it has been shown that the combination of MRSI and DWI has significantly higher accuracy than does MRSI alone in differentiating benign from malignant voxels in the peripheral zone (44). DWI appears to be particularly effective in detecting recurrent disease after radiation therapy or surgery.

DCE-MRI is a technique that uses small molecular weight gadolinium chelates for imaging tissue vascularity. Depending on the technique used, data reflecting tissue perfusion, microvessel permeability and extracellular leakage space can be obtained. Cancer often demonstrates nodular enhancement before the rest of the parenchyma and early washout of signal. This pattern is highly predictive of prostate cancer but not pathognomonic. Some prostate cancers are mildly or moderately hypervascular and are therefore not detectable with this method. Furthermore, angiogenesis is also present in benign prostatic hyperplasia and can be associated with prostatitis and premalignant changes, such as prostatic intraepithelial neoplasia (PIN) (45). Despite these limitations, DCE-MRI has been shown to have sensitivity of 73% and specificity of 81% in detecting prostate cancers (46). The addition of DCE-MRI to MRI or combined MRI/MRSI may further improve intraprostatic tumor localization. In a study of 34 patients, the accuracy levels (as measured by areas under receiver operating characteristic curves) for MRI, MRSI and DCE-MRI in prostate cancer localization were 0.68, 0.80, and 0.91, respectively (47).

MR lymphography with superparamagnetic nanoparticles has high sensitivity and specificity in depicting lymph node metastases (48). The inability of malignant nodal tissue to take up the agent provides tissue contrast within the lymph nodes. The technique has been used to detect small metastases (< 5 mm) as well as to differentiate between benign reactive and malignant enlarged nodes (48, 49). Although the technique appears promising, it is still restricted to the research setting in the United States.

Bone Scan and Positron Emission Tomography (PET)

The radionuclide bone scan continues to be the mainstay for diagnosing the initial spread of

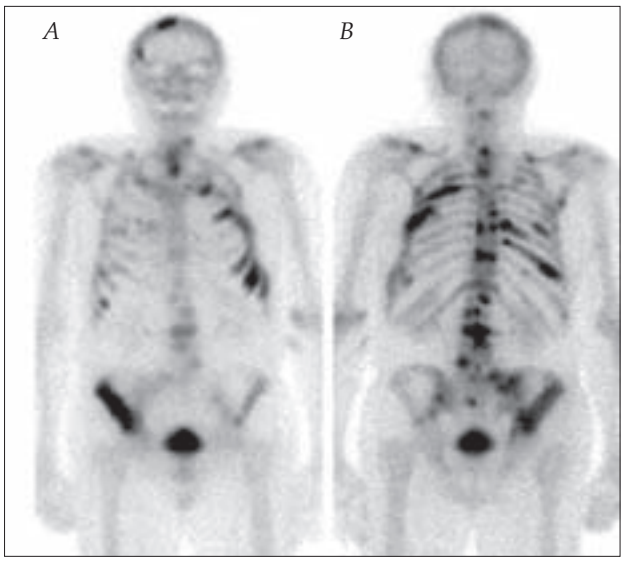

Figure 8. Radionuclide bone scintigraphy showing widespread metastasis in a patient with prostate cancer: (A) anterior view; (B) posterior view.

prostate cancer to the bone (Figure 8). It is generally reserved for patients with PSA > 10 ng/ml. Bone scanning can also be used to assess treatment response, as uptake usually decreases following radiotherapy, hormone therapy or chemotherapy. Single photon emission computed tomography (SPECT) studies of the skeleton have been shown to be more sensitive in the detection of metastatic disease than planar imaging (50, 51). A new technique, SPECT/CT, combines metabolic and anatomic information, though its incremental value has yet to be assessed.

PET imaging with the glucose analogue [^{18}F] 2-fluoro-D-deoxy-glucose (18F-FDG) in prostate cancer is challenging because glucose utilization in well-differentiated prostate cancer is often low and there is considerable overlap of uptake between prostate cancer, benign prostatic hyperplasia and inflammation. Generally, ^{18}F-FDG PET has been found to have low sensitivity for detecting primary prostate cancer (33) except in patients with advanced-stage and more aggressive disease (52). Limited data suggest that ^{18}F-FDG-PET/CT may have utility in the search for prostate cancer metastases after treatment, especially in aggressive and/or castration-resistant disease. In a study of 91 patients with PSA relapse after radical prostatectomy, ^{18}F-FDG PET detected disease in 28 patients (31%); it appeared to be useful in patients with PSA > 2.4 ng/mL or PSA doubling time > 1.3

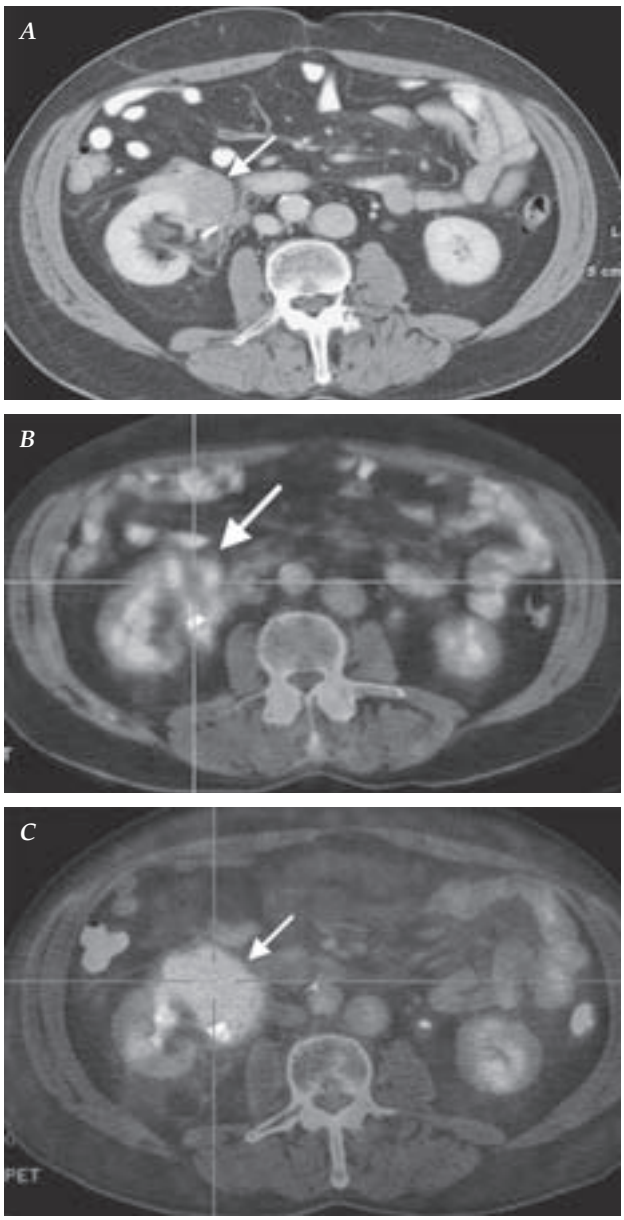

Figure 9. Comparison of CT and PET images of a single mass in a patient with prostate cancer. CT image (A) shows a soft-tissue mass (arrow). On ^{18}F-FDG PET (B) the mass (arrow) shows no tracer uptake. However, on ^{18}F-FDHT PET (C), the mass (arrow) shows marked tracer uptake.

ng/mL/y. Nearly all sites of disease detected by CT and bone scanning were detected with a single whole-body ^{18}F-FDG PET scan) (53).

New tracers that have shown promise for the detection of prostate cancer include carbon 11 (^{11}C) choline, uptake of which is increased in malignant tissue due to increased synthesis of membranal

phosphatidylcholine in tumor cells (54); ^{11}C acetate, which assesses oxidative metabolism in the tissue; and ^{11}C methionine, which differentiates tumor from normal tissue due to elevated protein synthesis (55). Other molecules in prostate cancer that can be detected using PET include androgen receptor, which can be targeted with ^{18}F-fluorodihydrotestosterone (FDHT), and prostate-specific membrane antigen (PSMA), which can be targeted with several different radiolabeled antibodies. The use of multiple tracer studies on the same patient often displays the heterogeneity of tumor biology. For example, patients who receive ^{11}C-methionine and ^{18}F-FDG PET scans on the same day may display metastases that are positive by both tracers, or that are positive by ^{11}C-methionine only or 18F-FDG only (56). Similarly, findings from ^{18}F-FDG-PET and ^{18}F-FDHT-PET may not match, suggesting variations in the androgen dependence of different disease sites (Figure 9).

The use of hybrid PET/CT helps identify the exact location of tracer uptake. With further research in molecular imaging, the number of targets for prostate cancer imaging is likely to increase.

Conclusion

At present, MR imaging is the modality of choice for the localization of primary prostate cancer. MRI, CT, bone scanning and PET have applications in the search for advanced or metastatic disease. Different imaging modalities have specific advantages and disadvantages, and thus the selection of an imaging modality should be based on the questions that need to be answered for a particular patient. Approaches that combine anatomical, functional and molecular data enable better disease characterization and are likely to play an increasingly important role in prostate cancer management.

REFERENCES

1. Motzer RJ, Russo P, Nanus DM et al. Renal cell carcinoma. Curr Probl Cancer 1997;21:185-232.
2. McLaughlin JK, Lindblad P, Mellemgaard A et al. International renal-cell cancer study. I. Tobacco use. Int J Cancer 1995;60:194-8.
3. Ficarra V, Prayer-Galetti T, Novella G et al. Incidental detection beyond pathological factors as prognostic predictor of renal cell carcinoma. Eur Urol 2003;43: 663-9.
4. Reuter VE, Presti JC. Contemporary approach to the classification of renal epithelial tumors. Semin Oncol 2000; 27:124-37.
5. Motzer RJ, Bander NH, Nanus DM. Renal-cell carcinoma. N Engl J Med 1996; 335:865-75.
6. Zangh J, Lefkowitz RA, Bach A. Imaging of kidney cancer. Radiol Clin North Am 2007;45:119-47.
7. Raj GV, Bach AM, Iasonos A et al. Predicting the histology of renal masses using preoperative Doppler ultrasonography. J Urol 2007;177:53-8.
8. Pallwein L, Mitterberger M, Aigner F et al. Small renal masses: the value of contrast-enhanced colour Doppler imaging. BJU Int 2007;99:579-85.
9. Zhang J, Lefkowitz R, Ishill N et al. Solid renal cortical tumors: differentiation with CT. Radiology Radiology 2007;244:494-504.
10. Jinzaki M, Tanimoto A, Mukai M et al. Double-phase helical CT of small renal parenchymal neoplasms: correlation with pathologic findings and tumor angiogenesis. J Comput Assist Tomogr 2000;24:835-42.
11. Herts BR, Coll DM, Novick AC et al. Enhancement characteristics of papillary renal neoplasms revealed on triphasic helical CT of the kidney. AJR Am J Roentgenol 2002;178:367-72.
12. Catalano C FF, Laghi A, Napoli A et al. High-resolution multidetector CT in the preoperative evaluation of patients with renal cell carcinoma. AJR Am J Roentgenol 2003;180:1271-7.
13. Studer UE, Scherz S, Scheidegger J et al. Enlargement of regional lymph nodes in renal cell carcinoma is often not due to metastases. J Urol 1990; 144:243-5.
14. Dighe M, Takayama T, Bush WH Jr. Preoperative planning for renal cell carcinoma--benefits of 64-slice CT imaging. Int Braz J Urol 2007;33:305-12.
15. Semelka RC, Shoenut JP, Kroeker MA et al. Renal lesions: controlled comparison between CT and 1.5-T MR imaging with nonenhanced and gadolinium-enhanced fat-suppressed spin-echo and breath-hold FLASH techniques. Radiology 1992;182:425-30.
16. Scialpi M, Di Maggio A, Midiri M et al. Small renal masses: assessment of lesion characterization and vascularity on dynamic contrast-enhanced MR imaging with fat suppression. AJR Am J Roentgenol 2000;175: 751-7.
17. Eilenberg SS, Lee JK, Brown J et al. Renal masses: evaluation with gradient-echo Gd-DTPA enhanced dynamic MR imaging. Radiology 1990;176:333-8.
18. John G, Semelka RC, Burdeny DA et al. Renal cell cancer: incidence of hemorrhage on MR images in patients with chronic renal insufficiency. J Magn Reson Imaging 1997;7:157-60.
19. Fein AB, Lee JK, Balfe DM et al. Diagnosis and staging of renal cell carcinoma: a comparison of MR imaging and CT. AJR Am J Roentgenol 1987;148:749-53.
20. Roy C, Sauer B, Lindner V et al. MR Imaging of papillary renal neoplasms: potential application for charac-

terization of small renal masses. Eur Radiol 2007;17: 193-200.
21. Israel GM, Hindman N, Bosniak MA. Evaluation of cystic renal masses: comparison of CT and MR imaging by using the Bosniak classification system. Radiology 2004;231:365-71.
22. Bouchelouche K, Oehr P. Positron emission tomography and positron emission tomography/computerized tomography of urological malignancies: an update review. J Urol 2008;179:34-45.
23. Divgi CR, Pandit-Taskar N, Jungbluth AA et al. Preoperative characterisation of clear-cell renal carcinoma using iodine-124-labelled antibody chimeric G250 (124I-cG250) and PET in patients with renal masses: a phase I trial. Lancet Oncol 2007;8:304-10.
24. Onik G. Percutaneous image-guided prostate cancer treatment: cryoablation as a successful example. Tech Vasc Interv Radiol. 2007;10:149-58.
25. Allsbrook WCJr, Mangold KA, Yang X et al. The Gleason grading system: an overview. J Urol Pathol 1999; 10:141-57.
26. Gleason DF, Mellinger GT. Prediction of prognosis for prostatic adenocarcinoma by combined histological grading and clinical staging. J Urol 1974;111:58-64.
27. Gonzalgo ML, Patil N, Su LM et al. Minimally invasive surgical approaches and management of prostate cancer. Urol Clin North Am 2008;35:489-504.
28. Zelefsky MJ, Yamada Y, Cohen G et al. Postimplantation dosimetric analysis of permanent transperineal prostate implantation: improved dose distributions with an intraoperative computer-optimized conformal planning technique. Int J Radiat Oncol Biol Phys 2000;48:601-8.
29. Heijmink SW, Barentsz JO. Contrast-enhanced versus systematic transrectal ultrasound-guided prostate cancer detection: an overview of techniques and a systematic review. Eur J Radiol 2007;63:310-6.
30. Pallwein L, Mitterberger M, Pelzer A et al. Ultrasound of prostate cancer: recent advances. Eur Radiol 2008; 18:707-15.
31. Salomon G, Köllerman J, Thederan I et al. Evaluation of prostate cancer detection with ultrasound real-time elastography: a comparison with step section pathological analysis after radical prostatectomy. Eur Urol 2008;54:1354-62.
32. O'Dowd GJ, Veltri RW, Orozco R et al. Update on the appropriate staging evaluation for newly diagnosed prostate cancer. J Urol 1997;158:687-98.
33. Hricak H, Choyke PL, Eberhardt SC et al. Imaging prostate cancer: a multidisciplinary perspective. Radiology 2007; 243 (1): 28-53. Erratum in: Radiology. 2007; 245(1):302.
34. Taoka T, Mayr NA, Lee HJ et al. Factors influencing visualization of vertebral metastases on MR imaging versus bone scintigraphy. AJR Am J Roentgenol 2001; 176:1525-30.
35. Mullerad M, Hricak H, Kuroiwa K et al. Comparison of endorectal magnetic resonance imaging, guided prostate biopsy and digital rectal examination in the preoperative anatomical localization of prostate cancer. J Urol. 2005;174:2158-63.
36. Sella T, Schwartz LH, Swindle PW et al. Suspected local recurrence after radical prostatectomy: endorectal coil MR imaging. Radiology 2004;231:379-85.
37. Jung JA, Coakley FV, Vigneron DB et al. Prostate depiction at endorectal MR spectroscopic imaging: investigation of a standardized evaluation system. Radiology 2004;233:701-8.
38. Scheidler J, Hricak H, Vigneron DB et al. Prostate cancer: localization with three-dimensional proton MR spectroscopic imaging – clinicopathologic study. Radiology 1999;213:473-80.
39. Shukla-Dave A, Hricak H, Moskowitz C et al. Detection of prostate cancer with MR spectroscopic imaging: an expanded paradigm incorporating polyamines. Radiology 2007;245:499-506.
40. Zakian KL, Sircar K, Hricak H et al. Correlation of proton MR spectroscopic imaging with gleason score based on step-section pathologic analysis after radical prostatectomy. Radiology 2005;234:804-14.
41. Hosseinzadeh K, Schwarz SD. Endorectal diffusion-weighted imaging in prostate cancer to differentiate malignant and benign peripheral zone tissue. J Magn Reson Imaging 2004;20:654-61.
42. Sato C, Naganawa S, Nakamura T et al. Differentiation of noncancerous tissue and cancer lesions by apparent diffusion coefficient values in transition and peripheral zones of the prostate. J Magn Reson Imaging 2005;21:258-62.
43. Haider MA, van der Kwast TH, Tanguay J et al. Combined T2-weighted and diffusion-weighted MRI for localization of prostate cancer. AJR Am J Roentgenol 2007;189:323-8.
44. Mazaheri Y, Shukla-Dave A, Hricak H et al. Prostate cancer: identification with combined diffusion-weighted MR imaging and 3D 1H MR spectroscopic imaging--correlation with pathologic findings. Radiology 2008;246:480-8.
45. Alonzi R, Padhani AR, Allen C. Dynamic contrast enhanced MRI in prostate cancer. Eur J Radiol 2007; 63:335-50.
46. Jager GJ, Ruijter ET, van de Kaa CA et al. Dynamic TurboFLASH subtraction technique for contrast-enhanced MR imaging of the prostate: correlation with histopathologic results. Radiology 1997;203:645-52.
47. Futterer JJ, Heijmink SW, Scheenen TW et al. Prostate cancer localization with dynamic contrast-enhanced MR imaging and proton MR spectroscopic imaging. Radiology 2006;241:449-58.
48. Harisinghani MG, Barentsz J, Hahn PF et al. Noninvasive detection of clinically occult lymph-node metastases in prostate cancer. N Engl J Med 2003;348:2491-9. Erratum in: N Engl J Med. 2003;2349(2410):1010.
49. Heesakkers RA, Futterer JJ, Hovels AM et al. Prostate cancer evaluated with ferumoxtran-10-enhanced T2*-weighted MR Imaging at 1.5 and 3.0 T: early experience. Radiology 2006;239:481-7.

50. Delpassand ES, Garcia JR, Bhadkamar V et al. Value of SPECT imaging of the thoracolumbar spine in cancer patients. Clin Nucl Med 1995;20:1047-51.
51. Even-Sapir E, Martin RH, Barnes DC et al. Role of SPECT in differentiating malignant from benign lesions in the lower thoracic and lumbar vertebrae. Radiology 1993;187:193-8.
52. Oyama N, Akino H, Suzuki Y et al. Prognostic value of 2-Deoxy-2-[F-18]-D-glucose positron emission tomography imaging for patients with prostate cancer. Mol Imaging and Biology 2002;4:99-104.
53. Schöder H, Herrmann K, Gönen M et al. 2-[18F]fluoro-2-deoxyglucose positron emission tomography for the detection of disease in patients with prostate-specific antigen relapse after radical prostatectomy. Clin Cancer Res 2005;11:4761-9.
54. Mishani E, Ben-David I, Rozen Y. Improved method for the quality assurance of [C-11]choline. Nucl Med Biol 2002; 29:359-62.
55. Jager PL, Vaalburg W, Pruim J et al. Radiolabeled amino acids: basic aspects and clinical applications in oncology. J Nucl Med 2001;42:432-45.
56. Nunez R, Macapinlac HA, Yeung HW et al. Combined 18F-FDG and 11C-methionine PET scans in patients with newly progressive metastatic prostate cancer. J Nucl Med 2002;43:46-55.

Author's address: Hedvig Hricak, MD, PhD, Dr hc, Chairman, Department of Radiology Memorial Sloan-Kettering Cancer Center, 1275 York Avenue, room C-278, New York, NY 10065, USA; E-mail: hricakh@mskcc.org